NIH Public Access
Author Manuscript
J Am Chem Soc. Author manuscript; available in PMC 2014 October 23.

Published in final edited form as:
J Am Chem Soc. 2013 October 23; 135(42): . doi:10.1021/ja406696k.

Dipalladium(I) Terphenyl Diphosphine Complexes as Models for Two-Site Adsorption and Activation of Organic Molecules

Sibo Lin, **David E. Herbert**, **Alexandra Velian**, **Michael W. Day**, and **Theodor Agapie***
Department of Chemistry and Chemical Engineering, California Institute of Technology, 1200 East California Boulevard MC127-72, Pasadena, California 91125, United States

Abstract

Well-defined models for binding of organic molecules across two metal centers are relatively rare. A paraterphenyl diphosphine was employed to support a dipalladium(I) moiety. Unlike previously reported dipalladium(I) species, the present system provides a single molecular hemisphere for binding of ligands across two metal centers, enabling the characterization and comparison of the binding of a wide variety of saturated and unsaturated organic molecules. The dipalladium(I) terphenyl diphosphine toluene-capped complex was synthesized from a dipalladium(I) hexaacetonitrile precursor in the presence of toluene. The palladium centers display interactions with the π-systems of the central ring of the terphenyl unit and that of the toluene. Exchange of toluene for anisole, 1,3-butadiene, 1,3-cyclohexadiene, thiophenes, pyrroles, or furans resulted in well-defined π-bound complexes which were studied by crystallography, nuclear magnetic resonance (NMR) spectroscopy, and density functional theory. Structural characterization shows that the interactions of the dipalladium unit with the central arene of the diphosphine does not vary significantly in this series allowing for a systematic comparison of the binding of the incoming ligands to the dipalladium moiety. Several of the complexes exhibit rare μ^2-η^2:η^2 or μ^2-η^2:η^1 (*O* or *S*) bridging motifs. Hydrogenation of the thiophene and benzothiophene adducts was demonstrated to proceed at room temperature. The relative binding strength of the neutral ligands was determined by competition experiments monitored by NMR spectroscopy. The relative equilibrium constants for ligand substitution span over 13 orders of magnitude. This represents the most comprehensive analysis to date of the relative binding of heterocycles and unsaturated ligands to bimetallic sites. Binding interactions were computationally studied with electrostatic potentials and molecular orbital analysis. Anionic ligands were also demonstrated to form π-bound complexes.

1. Introduction

The majority of organometallic studies have focused on mononuclear compounds, but reactions at surfaces, clusters, and homogeneous catalysts may involve multiple metal centers. Reactions involving aromatic systems such as hydrogenation or cross-coupling often invoke intermediates with the π-systems coordinating to one or more metals on the surface.[1-3] Additionally in petroleum refining, removal of sulfur and nitrogen impurities (hydrodesulfurisation and hydrodenitrification, respectively) requires binding and activation of nitrogen and sulfur-containing heterocycles.[4] Heteroatom-containing molecules are known to inhibit these processes,[5] but very few organometallic models for multinuclear

***Corresponding Author**agapie@caltech.edu.

SUPPORTING INFORMATION AVAILABLE Experimental procedures, figures, tables of NMR and crystallographic data, and computational details. This material is available free of charge via the Internet at http://pubs.acs.org.

Notes The authors declare no competing financial interests.

NIH-PA Author Manuscript
NIH-PA Author Manuscript
NIH-PA Author Manuscript

NIH-PA Author Manuscript

NIH-PA Author Manuscript

NIH-PA Author Manuscript

binding of heterocycles are known.[6] In this context, structural models and quantitative evaluation of binding with π-interactions and heteroatoms to multimetallic sites are of interest.

The Pd(I)-Pd(I) moiety with a metal-metal σ-bond has been shown to be stable without support from bridging ligands and binds a variety of π-systems.[7-9] Numerous homogeneous dinuclear palladium complexes displaying bridging arenes,[10-18] butadienes,[19-21] allyls[22-27], and recently pyrroles[5] have been reported (Chart 1). In these complexes there is significant variation in the nature of the ancillary ligands (L, L', X). This is due to the mode of synthesis that typically coordinates two identical π-systems to a Pd_2 unit. We have designed a diphosphine supporting ligand that allows for systematic studies of single ligand binding to a Pd_2 unit (Figure 1, right).

Herein, we report the synthesis of dipalladium(I) complexes supported by a common π-terphenyl diphosphine framework. This platform has been synthesized with capping arenes, heterocycles, and other organic ligands. The coordination modes, dynamic processes, relative binding strengths, and reactivity were investigated by single crystal X-ray diffraction (XRD), solution nuclear magnetic resonance spectroscopy (NMR), and density functional theory (DFT) calculations. The present study provides insight into the coordination of common ligands spanning a relative binding window of over 13 orders of magnitude.

2. Results and Discussion

2.1. Synthesis and Characterization of Arene Adducts

Terphenyl diphosphines have been employed as trans-spanning ligands for supporting mono- and bimetallic complexes.[28-31] In particular, diphosphine **1** (Scheme 1) was shown to coordinate a Ni^{I}-Ni^{I} moiety with phosphine coordination roughly along the metal-metal vector.[28] The central arene was found to have interactions with the metal centers and to coordinatively and sterically saturate one hemisphere of the bimetallic unit. An analogous motif was targeted for palladiumd.

The M^{II}/M^{0} *in situ* comproportionation reaction, employed for nickel, was not successful for palladium. An alternate synthetic strategy was tested, utilizing preformed dipalladium precursor $[Pd_2(MeCN)_6][BF_4]_2$ (**2**).[7] As the two reagents are not soluble in the same solvents, a solution of **2** in MeCN was added to solid diphosphine **1** with rapid stirring. The initial dark red suspension became more homogeneous after stirring for ~10 minutes. Upon removal of volatile materials, the dark red residue was recrystallized by reconstitution with CH_2Cl_2 and layering under toluene to give toluene adduct **3** (Scheme 1).

^{1}H NMR spectra of these crystals in CD_2Cl_2 displayed a singlet and a multiplet significantly upfield from the aromatic region (6.21 and 6.19 ppm, respectively). The singlet was assigned to the protons of the central arene of the terphenyl backbone. The chemical shift suggests coordination of the π-system of the central arene to the palladium centers, as previously observed for the nickel analogs.[28] ^{1}H-^{13}C 2D NMR experiments (HSQC and HMBC) identified the multiplet as corresponding to a bound toluene molecule. The carbons *ortho*-, *meta*-, and *para*- to the toluene methyl are shielded (104.7, 91.3, and 100.9 ppm, respectively), consistent with π-coordination to a metal center and disruption of aromaticity. The methyl group of toluene is expected to be located away from the P-P vector due to steric reasons, which would make the molecule pseudo-C_s symmetric and show two peaks for the central arene in the slow exchange limit. The observation of a singlet for the central arene protons indicates a fast exchange process on the NMR time scale that involves the toluene ligand. Addition of excess toluene to an NMR sample of **3** allowed observation of peaks

NIH-PA Author Manuscript

NIH-PA Author Manuscript

NIH-PA Author Manuscript

corresponding to bound and free toluene instead of an averaged spectrum, indicating that degenerate ligand substitution is slow on the NMR timescale. These findings are consistent with the toluene rotating 180° on the NMR time scale. Additionally, the Pd_2 unit exchanges fast between coordination to π-electrons in the "front" and "back" (as drawn) of the central ring (eq 1).

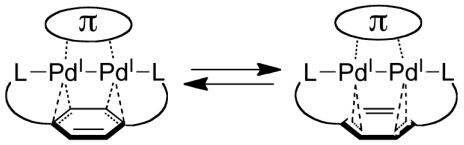

(1)

Crystals of **3** were further studied by XRD (Figure 1). The two palladium(I) centers are sandwiched between the central ring of the terphenyl backbone and a capping toluene molecule. The central ring is bound μ-η^2:η^2 through two adjacent, partially localized double bonds. These central arene bonds are elongated (1.409(3) and 1.420(3) Å), while the third, uncoordinated double bond of the central ring is noticeably shorter (1.360(2) Å) relative to a typical aromatic C-C bond. The toluene molecule is bound μ-η^2:η^2 (using a Pd-C cutoff distance of 2.5 Å to assign bonds), and two phosphines complete the coordination sphere. The terphenyl unit adopts a convex geometry to accommodate the bimetallic core. Interestingly, the Pd–Pd distance of 2.7091(2) Å is a close match for nearest-neighbor Pd–Pd distances of bulk Pd (2.75 Å).[32,33]

^{1}H NMR spectra in CD3CN revealed the lability of toluene from **3**. A new singlet at 5.96 ppm is assigned as the central arene protons. Peaks corresponding to free toluene[35] are also observed. Dissolution of **3** in CH_3CN followed by removal of volatiles under vacuum shows by ^{1}H NMR analysis (CD_2Cl_2) that the toluene has been exchanged for two acetonitrile ligands (2.56 ppm, *cf.* 1.97 ppm for free CH_3CN in CD_2Cl_2[35]).

Furthermore, layering of this acetonitrile-capped species in DCM under anisole yielded red crystals of anisole-capped species **4** (Scheme 1). XRD analysis revealed a π-binding mode similar to that of toluene (Figure 1). In the solid-state, the methoxy group is nearly coplanar with the anisole ring (dihedral angle, ϕ = 3°). The π-coordination of anisole in solution is supported by NMR spectra (CD_3NO_2) of **4** exhibiting features analogous to those of **3**: ^{1}H NMR olefinic singlet and multiplet (6.21 and 5.96 ppm, respectively) and shielded *ortho*-, *meta*-, and *para*-^{13}C NMR anisole signals (86.7, 94.7, and 87.4 ppm).

2.2. Synthesis and Characterization of Diene Adducts

The lability of toluene in **3** raised the question if neutral non-aromatic dienes or diene analogues could serve as more strongly binding ligands. Upon exposure of **3** to 1 atm of 1,3-butadiene (Scheme 1), the reaction mixture became light orange. Light yellow crystals of the resultant species **5** were obtained from acetonitrile solution layered under diethyl ether (Et_2O), and XRD revealed a μ-η^2:η^2-(s-*trans*)-butadiene capping two Pd centers that are 2.8379(8) Å apart (Figure S64). This motif mirrors that proposed for 1,3-butadiene on Pd(110) between nearest-neighbor surface atoms based on STM image analysis.[36] The Pd–Pd distance enforced by the terphenyl framework contrasts with a Pd–Pd separation of 3.19 Å reported for a bis(butadiene) sandwich.[19] The present Pd–Pd distance is closer to that in one atom-bridged systems (Figure 1, bottom left, X = halide, r(Pd–Pd) = 2.58 to 2.70 Å),[20,37] suggesting that the terphenyl diphosphine compresses the distance between the two metals.

NIH-PA Author Manuscript

NIH-PA Author Manuscript

NIH-PA Author Manuscript

While crystallographic disorder of the butadiene ligand[38] obscures accurate determination of the structural parameters corresponding to bonding with the metal centers, the NMR data provides information about the dynamics of the Pd_2-butadiene interaction in solution. The central arene protons of **5** are represented by two ^{1}H NMR doublets (δ = 6.10, 5.83 ppm; J = 7.8 Hz). One ^{31}P NMR peak (δ = 78.8 ppm) is observed. These observations are consistent with the pseudo-C_2 symmetric solid-state structure persisting in solution on the NMR timescale, indicating that the Pd_2 unit exchanges fast relative to the central ring (eq 1). The diene binding, however, is not fluxional on the NMR time scale. The lack of butadiene displacement by MeCN is consistent with the plethora of stable s-*trans*-diene-bridged dipalladium compounds in the literature.[19,20,39]

In contrast, 1,3-cyclohexadiene (CHD), an s-*cis*-diene, has rarely been isolated bridging between two adjacent metal centers.[19,20] No crystal structures have been published previously. The present terphenyl diphosphine framework was thus employed to characterize such an adduct. Addition of 10 equiv. CHD to a CD_3CN solution of **3** formed a new species (**6**) nearly quantitatively within minutes (Scheme 1). By ^{1}H NMR spectroscopy, **6** exhibits two singlets (6.35, 5.45 ppm) and one multiplet (4.78 ppm) in the olefinic region, all with approximately the same integration. A ^{1}H-^{1}H 2D NMR experiment (COSY) showed the multiplet being correlated with a second multiplet at 7.18 ppm. The olefinic singlets are attributed to the central arene, and the multiplets are assigned to CHD.[40] This data is consistent with a μ-η^2:η^2-CHD adduct in solution, where rotation of the CHD adduct atop the two metal centers and CHD dissociation are slow on the NMR time scale. Similar to butadiene, these suggest that the interaction with the diene moiety is strong. Yellow crystals were grown via vapor diffusion of Et_2O into a MeCN solution of **6**, and an XRD study yielded the structure suggested by NMR data, albeit with significant disorder (Figure S65). This is the first reported structure of CHD bound to any dipalladium moiety. While no surface studies of CHD adsorption on Pd have been reported, a study of CHD adsorption on Pt(111) predicted the present μ^2 motif to be unstable and a μ^3 binding mode to be lower in energy.[41] However, the present motif may be important on lower coordinate faces [e.g. (110), (210), etc.] and defect sites.

2.3. Synthesis and Characterization of Heterocycle Adducts

The well-defined ligation of olefins and arenes indicated that the dipalladium moiety supported by terphenyl diphosphine, **1**, may allow for binding of a much broader spectrum of substrates. Dipalladium species bridged by thiophenes, pyrroles, and furans were explored.

2.3.1 Thiophenes—Adding 10 equivalents of thiophene to a red solution of **3** in CD^3CN did not result in any changes observable by NMR spectroscopy. To limit competitive binding from excess acetonitrile, reaction in CH_2Cl_2 was attempted, but found to be slow due to the low solubility of **3**. Thus, **3** was first treated with acetonitrile to exchange away toluene, then volatiles were removed under vacuum. This material readily dissolved in CH_2Cl_2 and reacted upon addition of excess thiophene, resulting in orange precipitate of **7** within seconds (Scheme 1). XRD-quality crystals of **7** were grown by diffusion of Et_2O vapor into a nitromethane solution (Figure 1). In the solid-state, thiophene is μ-η^2:η^2-bound, with the C=C double bonds (1.401(1), 1.404(1) Å) and the C–S bonds (1.7535(9) and 1.7484(9) Å) elongated relative to free thiophene.[42] These metrics suggest that aromaticity in thiophene is disrupted by the interaction of the metal centers with the double bonds. While mononuclear adducts of η^2-thiophene are well-known[43-47] and higher hapticity mononuclear adducts have precedent,[48-51] dinuclear adducts of thiophene are rare. In most examples, cleavage of a C–S bond occurs (perhaps through a mononuclear intermediate) and polynuclear adducts of C–S cleaved fragments are observed.[52-54] In the nearest precedent to

NIH-PA Author Manuscript

NIH-PA Author Manuscript

NIH-PA Author Manuscript

7, 3,4-bis(trifluoromethyl)-S-methyl-thiophenium was reported to be μ-η^2:η^2-bound to a dimolydenum moiety.[55]

Nickel and palladium have been extensively used to cross-couple thiophene groups, but prior to **7**, no π-adducts were structurally characterized. Organonickel thiophene π-adducts have been proposed to play a role in various processes, such as precursors to C-S oxidative addition[56] and propagating species in nickel-catalyzed polymerization of 3-alkylthiophenes.[57] Analogous thiophene π-adducts in organopalladium chemistry have yet to be documented.

EXAFS studies have found thiophene monolayers to bind parallel to Pd(111) and (100) surfaces.[58] The initially proposed adsorption models had the carbons bound essentially η^4-atop one Pd center with unusually long Pd–C bonds (>2.5 Å c.f. ~2.16 Å in $Pd(COD)_2$[59]). A later DFT study of thiophene on Pd(100) explored six adsorption geometries and found an energy minimum with the double bonds bridging three metal centers and sulfur binding a fourth metal center.[60] A thiophene-surface adsorption model in which the double bonds are μ^2-η^2:η^2-bound to two Pd centers, as in **7**, has never been discussed in the literature, to the best of our knowledge.[61]

To determine the effect of substitution on the thiophene binding mode, the synthesis of 2-methylthiophene and 3-methylthiophene complexes was attempted. Analogous procedures to that for thiophene afforded XRD-quality crystals of **8** and **9**, respectively (Scheme 1). 3-Methylthiophene in **9** is μ-η^2:η^2-bound, similar to thiophene in **7**, but 2-methylthiophene in **8** is μ-η^2:η^1(S)-bound (Figure 1). Prior to this work, this latter cofacial bridging mode of thiophene had not been crystallographically characterized and nor analyzed in computational studies of thiophene on metal surfaces. The only previously reported co-facial μ-η^2:η^1(S)-heterocycle adducts were enforced by C-H activation of the 2-position by a third metal center in a triosmium cluster.[62,63] The observed differences in the binding modes are likely due to the steric interactions. Binding of 2-methylthiophene similar to thiophene would direct the methyl group toward the isopropyl substituents. The methyl group of 3-methylthiophene, however, does not have unfavorable steric interactions and thus binds like thiophene.

To examine the persistence and fluxionality of these binding modes in solution, **7**-**9** and 2,5-dimethylthiophene adduct **10** were studied by NMR spectroscopy (CD_3NO_2, 25 °C). Atypical ^{1}H chemical shifts attributed to the thiophene moiety in **7** are similar to those attributed to olefinic protons of π-bound CHD in **6**.[40,64] Compounds **7**-**10** each exhibit a ^{1}H NMR peak between 6.25 and 6.11 ppm corresponding to the four equivalent central arene protons, but the shape of this peak at room temperature varies from a sharp singlet (full width at half maximum (FWHM) ~ 1 Hz) for **7** to a very broad peak (FWHM = 146 Hz) for **9**. ^{1}H NMR spectra of **7** collected at −20 °C show broadening of the central arene signal but not decoalescence into two peaks. This indicates that for **7**, fluxional processes occur rapidly on the NMR timescale, at room temperature, to generate pseudo-C_{2v} symmetry in solution. In contrast, for **9**, partial decoalescence of the central arene ^{1}H signal into two peaks is observed at −18 °C, and coalescence to a sharp ^{1}H singlet is observed only upon heating at 90 °C. While the lack of full decoalescence at temperatures above the solvent freezing point precludes precise calculation, ΔG‡ at 25 °C for fluxional processes in **9** is equal to or greater than 13 kcal/mol.

Two mechanisms may be responsible for the fluxional processes in π-coordinated thiophenes and other heterocycles (Scheme 2). The central arene of the diphosphine is assumed to exchange rapidly as discussed previously (eq 1). Additionally, “spinning” of the heterocycle may occur to exchange the atoms ligated to the metal centers. This mechanism

NIH-PA Author Manuscript

NIH-PA Author Manuscript

NIH-PA Author Manuscript

could also be responsible for the exchange processes in arenes in **3** and **4**. Alternatively, the binding mode of the heterocycle may change from the π-system to a dative interaction from the lone pairs on the heteroatom. Re-coordination, or "flipping", to the heterocycle π-system may result in a different orientation relative to the central arene. For heterocycles that have C_{2v} symmetry in free form (e.g. thiophene, 2,5-dimethylthiophene), both spinning and flipping mechanisms could account for observation of one singlet for the four central arene protons. However, for heterocycles with only C_s symmetry, the spinning mechanism could not make all four central ring protons equivalent. Therefore, flipping would be responsible for the exchange.

2.3.2. Pyrroles—Pyrrole and *N*-methylpyrrole adducts **11** and **12** were synthesized and isolated in an analogous procedure to **7** (Scheme 1). Both complexes exhibit two multiplets between 3.22 and 3.02 ppm and a downfield ^{1}H NMR multiplet (8.89 and 8.62 ppm, respectively). The two aliphatic multiplets correspond to two isopropyl methine environments and the downfield multiplet corresponds to the α-H nuclei (α-Hs) of the heterocycle. These features are consistent with a C_s-symmetric structure. Given that the 1- and 4-Hs in CHD adduct **6** and α-Hs of thiophene adduct **7** are also shifted conspicuously downfield (7.18 and 8.80 ppm, respectively), the binding modes of pyrrole and *N*-methylpyrrole are likely structurally analogous, i.e. μ^2-η^2:η^2.[64]

Dipalladium(I) complexes sandwiched by two μ-η^2:η^2-pyrroles were recently reported[6] but due to their high symmetry could not be easily used to elucidate the fluxionality of π-bound pyrroles. In **11** and **12**, the asymmetric sandwich motif facilitates the study of fluxional processes. The ^{1}H NMR spectrum of **11** displays central arene signals (6.24 and 6.15 ppm, FWHM = 8.4 Hz) that are broader than those of **12** (6.28 and 6.17 ppm, FWHM = 3.6 Hz), suggesting that pyrrole spinning occurs and is faster than ^{N}-methylpyrrole spinning. A variable temperature ^{1}H NMR study of **11** shows coalescence of the central arene signals and isopropyl methine signals near 50 °C. Flipping is not possible in this case, as the nitrogen center does not have an accessible lone pair in contrast to sulfur in thiophene.

2.3.3. Furans—Furan and 2-methylfuran adducts **13** and **14** were accessed in a procedure analogous to **7** (Scheme 1). The ^{1}H NMR spectrum of **13** exhibits two doublets in the olefinic region (6.32, 6.27 ppm; J = 1.4 Hz) and two multiplets downfield and upfield of the aromatic region (9.42, 6.41 ppm, respectively), all with approximately the same integration. 40 These features, mirroring those of **6** and **12**, suggest that furan is μ-η^2:η^2-bound and not rapidly fluxional on the NMR timescale. In contrast, 2-methylfuran adduct **14** exhibits three ^{1}H NMR multiplets between 6.38 and 6.08 ppm (integrating 2:1:1) and ^{31}P NMR doublets at 60.9 and 57.4 ppm (J_{pp} = 162 Hz). The ^{1}H NMR multiplets, corresponding to the central arene protons, and the asymmetric phosphines support a time-averaged C_1-symmetric structure for **14**. Such a structure could be realized with μ-η^2:η^2 or μ-η^2:η^1(O) binding modes for 2-methylfuran. Given the large difference in ^{13}C NMR chemical shift between the α-Cs of the bound heterocycle (O*C*CH$_3$ = 179.8; O*C*H = 65.5 ppm), μ-η^2:η^1(O) binding was initially suspected. However, XRD study of **14** revealed a μ-η^2:η^2 binding mode (Figure 1). Asymmetric binding of the α-Cs (Δr(Pd-C) = 0.24 Å) may account for their dissimilar chemical shifts. Theoretical studies of furan on Pd(111) surfaces indicated low-energy binding modes across three metal centers,[65] but the μ^2-η^2:η^2 motif from **13** and **14** may be present on lower-coordinate surfaces. Such furan binding modes have not been crystallographically characterized previously, although trans-facial μ^2-η^2:η^2 binding of furan to two Re(I) centers has been proposed.[44]

To explore if furan spinning or flipping is thermally accessible, a variable temperature NMR study of **13** was conducted. The difference in chemical shift of the central arene peaks (Δδ)

NIH-PA Author Manuscript

NIH-PA Author Manuscript

NIH-PA Author Manuscript

was recorded near the freezing temperature of the NMR solvent (CD_3NO_2). From −25 °C to 90 °C, $\Delta\delta$ decreased from 0.11 to 0.02 ppm, suggesting that an exchange process occurs but is slow on the NMR timescale.

2.3.4. Benzo-derivatives: Benzothiophene, Indole, and 4,6-Dimethyldibenzothiophene—Perhaps due to the large number of surface conformations and atoms, theoretical adsorption models of benzothiophene and indole on surfaces have been less developed than for five-membered heterocycles. Thus, benzothiophene- and indole-bridged species **15** and **16** were synthesized, purified, and crystallized in an analogous manner to **7** (Scheme 1). XRD analysis reveals benzothiophene to be bound μ-η^2:η^1(S), whereas indole binds μ-η^2:η^2 through its carbocyclic ring (Figure 1). The only previously reported co-facial μ-η^2:η^1(S)-benzothiophene adducts were enforced by C-H activation of the 2-position by a third metal center in a trinuclear cluster,[62,63] but the all-carbon binding mode of indole in **16** mirrors that in a recently reported bisindole dipalladium(I) sandwich complex.**6**

The asymmetry of the present terphenyl diphosphine environment again allows analysis of the fluxionality of benzothiophene and indole ligands that would be difficult in a symmetric sandwich compound. At room temperature, ^{1}H NMR spectra of **15** exhibit four peaks spanning 5.75-6.13, and ^{31}P NMR spectra show doublets at 67.3 and 65.9 ppm (J = 168 Hz). In contrast, ^{1}H NMR spectra of **16** exhibits two broad peaks at 6.42 and 5.57 ppm, and ^{31}P NMR spectra show one broad peak at 64.7 ppm. The ^{1}H NMR features, attributed to the central arene protons, and the ^{31}P NMR spectra indicate that benzothiophene, bound through its heterocyclic ring, does not spin or flip rapidly on the NMR timescale, but indole, bound through its carbocyclic ring, may be able to rapidly spin on the NMR timescale. Coincidental overlap of the central arene ^{1}H and phosphine ^{31}P signals, rather than fast exchange processes, could not be ruled out.

4,6-Dimethyldibenzothiophene is considered to be an especially recalcitrant heterocycle toward hydrodesulfurization.[66] Crystallographically characterized models for multinuclear binding have not been previously reported. Targeting such a model, 4,6-dimethyldibenzothiophene adduct **17** was synthesized and studied (Figure 2). XRD analysis show that the heterocycle is bound μ^2-S, perpendicular relative to the central arene, in contrast to the parallel heterocycles in **7-16**. The S-C bonds are elongated 0.02 Å relative to free 4,6-dimethyldibenzothiophene.[67] This is the first crystallographically characterized example of a μ^2-S bound dibenzothiophene. The structure has pseudo-C_{2v} symmetry, with the central arene coordinated μ-(η^3, η^3), compared to the μ-(η^2, η^2) binding mode observed for the other complexes. This difference may be due to the steric constraints imposed by the bulky 4,6-dimethyldibenzothiophene ligand hindering distortion to the μ-(η^2, η^2) coordnation, of C_s symmetry. The perpendicular binding mode is likely also the result of steric interactions with the ligand isopropyl groups for the parallel coordination; on a palladium surface, the methyl groups might interfere with perpendicular binding, and parallel π-coordination might be preferred. Perpendicular σ-binding is proposed to precede C-S bond cleavage in hydrodesulfurization over Ni-MoS_2/γ-Al_2O_3.[66]

2.3.5. Comparison of Fluxional Processes of S-, N-, and O-Heterocycle Adducts—In the above observations of compounds **7-14**, generally, the fluxionality of bound thiophenes is greater than bound pyrroles, which in turn are more fluxional than furans. Energetically similar Pd-heteroatom and Pd-(C=C) interactions are expected to lead to small barriers for fluxional processes depicted in Scheme 2. According to hard-soft acid-base theory,[68] sulfur is a soft, better-matched, ligand for palladium than nitrogen or oxygen. Thus, the spinning and flipping intermediates illustrated in Scheme 2 are expected to be more readily accessible for bound thiophene. In fact, the solid-state structures of **8**, **9**, and **15**

NIH-PA Author Manuscript

NIH-PA Author Manuscript

NIH-PA Author Manuscript

are models for spinning intermediates and that of **17** is a model for a flipping intermediate. Accordingly, the central arene and isopropyl methine protons of **7** appear as single resonances in room temperature ^{1}H NMR spectra. Nitrogen is a worse matched ligand than sulfur, and a μ^2-N flipping intermediate is not possible for pyrroles, which do not have a lone pair on the heteroatom that is not part of the π-system. Correspondingly, by ^{1}H NMR the central arene protons of **11** have coalesced to one peak, but the isopropyl methine protons remain two distinct peaks at room temperature. The apparent fluxionality of indole in **16** should be attributed to the fact that no Pd-N bond needs to be formed during spinning about the carbocyclic ring. Finally, oxygen is a hard Lewis base, and spinning or flipping intermediates displaying Pd-O bonds are expected to be prohibitively uphill. The relatively static behavior of furan in **13** and the μ^2-η^2:η^2 coordination mode of 2-methylfuran in **14**, despite steric repulsion from the isopropyl groups (*cf*. **8**), support this trend. Consistent with the above explanations, rings with higher aromaticity are expected to have lower barriers to exchange. In agreement, the order of aromaticity of heterocycles (thiophene > pyrrole > furan) matches the observed qualitative exchange rates.[69]

2.4 Hydrogenation of S-Heterocycle Adducts

Palladium has been explored as a component of next-generation deep hydrodesulfurization catalysts.[70,71] Initial π-coordination on Pd surfaces is proposed to facilitate subsequent cleavage of otherwise unreactive C–S bonds.[72,73] To study this process, **7** in CH_3NO_2 was sealed with 3.8 atm H2 in a J. Young NMR tube (Scheme 3). Over 5 h at room temperature, **7** was fully converted to a new species **18** by ^{31}P (δ = 69.8 ppm) and some black precipitate was formed. This species was precipitated from MeCN by addition of excess Et_2O and exhibited a singlet in the region for central arene protons and two new aliphatic multiplets (6.09, 3.55, and 2.43 ppm) integrating 1:1:1. Thus, **18** was assigned to contain one bridging tetrahydrothiophene (THT) ligand (97% isolated yield). The constitution of **18** was further confirmed by gas chromatography-mass spectrometry (GC-MS) of the reaction mixture, which showed a match for THT. An independent synthesis by addition of THT to **3** released toluene and directly formed **18** (Figure 3), supporting the above assignment. Under identical hydrogenation conditions, benzothiophene adduct **15** was observed to convert to a more symmetric species with one ^{31}P NMR signal (72.8 ppm, s), which could be a κS-dihydrobenzothiphene adduct. GC-MS of the reaction mixture confirmed the presence of 2,3-dihydrobenzothiophene. No intermediates were observed in significant amounts during these hydrogenation reactions. No hydrogenation/hydrogenolysis products were observed under similar reaction conditions with 4,6-dimethyldibenzothiophene adduct **17**.

Under hydrogenation conditions, small amounts of black precipitate were observed, suggesting some reduction to Pd(0). Hydrogenation of thiophene by heterogeneous palladium, which has previously been reported for η^2-thiophene tungsten compounds,[45] cannot be ruled out. However, the hydrogenation of free thiophene with heterogeneous palladium catalysts has been reported under strongly acidic conditions or at elevated temperatures.[74]. In the present system, the π-coordination of thiophene may activate it towards hydrogenation, although the exact mechanism is currently unclear.

2.5. Synthesis and Characterization of Anionic-Bridged Complexes

Bridging anionic allyl species have been proposed in hydrocracking and hydrogenation mechanisms on heterogeneous Pd[75] and have been recently discovered to exhibit reactivity toward CO_2 in a homogeneous system.[24,76] To test if such ligands could be supported on the present dipalladium motif, **3** was initially treated with sodium *n*-propanoate to form a red, putative carboxylate complex (**19**, Scheme 4). Subsequent transmetallation with tributylallyltin yielded a yellow species **20**, which exhibited two inequivalent central arene singlets (6.23, 5.55 ppm) in the ^{1}H NMR spectrum, suggesting slow or no rotation of the

NIH-PA Author Manuscript

NIH-PA Author Manuscript

NIH-PA Author Manuscript

bridging allyl on the NMR time scale. Crystals of **20** were grown from a CH3CN solution layered under Et_2O and analyzed by XRD. The solid-state structure shows the allyl moiety to bridge symmetrically the two metal centers (Figure 3).

A related heteroallyl species **21** was synthesized by reaction of **3** with KO^{t}Bu in MeCN (Scheme 4). NMR spectra of **21** showed broad ^{1}H peaks corresponding to the C*H* and CH_3 moieties (4.51 and 2.32 ppm) of an iminobutanenitrilyl anion and broad ^{31}P peaks at 50.2 and 49.2 ppm. FAB-MS found a major species with m/z = 757.1390 (calcd. BF_4-dissociated cation: 757.1132). Although **21** could not be isolated cleanly, its assignment was supported through an alternate synthesis by treating **3** with a pre-formed diacetonitrilyl anion.[77] Crystals grown from a CH_2Cl_2 solution layered under Et_2O were studied by XRD, and revealed the dipalladium moiety capped by a μ-κC:κN-NC*C*HC(CH_3)*N*H moiety (Figure 3). Such diacetonitrlyl anions have not structurally characterized in this particular tautomer or binding motif.[78] While the allyl carbons in **20** lie in a plane canted toward that of the central arene, the three atoms of the heteroallyl in **21** are tilted away from the central arene. (φ(allyl, central arene) = 20.6°; φ(heteroallyl, central arene) = −19.4°). Thus allyl binds μ-η^2:η^2, but diacetonitrilyl binds μ-κC:κN.

2.6. Experimentally Determined Relative Binding Strength of Ligands

The capping arenes, furans, and thiophenes in **3**, **4**, **7**-**10**, **13**-**15**, and **17** are all quantitatively displaced by acetonitrile (determined by ^{1}H NMR) upon dissolution of the compound in CD_3CN. In contrast, capping dienes, N-heterocycles, and THT in **5**, **6**, **11**, **12**, **16**, and **18** are persistent in CD_3CN. With access to this series of diverse, yet structurally related compounds we proceeded to measure the relative binding strengths of a variety of ligands to a Pd_2 moiety. To compare the binding of these ligands, equilibrium experiments starting with thiophene adduct **7** and a free diene, arene, or heterocycle were performed (eq 2):

$$[Pd_2P_2(\text{thiophene})]^{2+}\ (\mathbf{7}) + \text{ligand} \rightleftharpoons [Pd_2P_2(\text{ligand})]^{2+} + \text{thiophene} \quad (2)$$

All species (except for THT adduct **18**) in the equilibrium mixture did not exhibit peak shifting, broadening, or coalescence, which indicates slow intermolecular exchange on the NMR timescale. The relative concentrations were determined by integration of ^{1}H NMR spectra (CD_3NO_2, 25 °C). The resulting equilibrium constants were found to span greater than 13 orders of magnitude (Figure 4). To our knowledge, this is the first study that has allowed the measurement of quantitative binding affinities of such a broad class of substrates relevant to many catalytic transformations involving π-systems.[79] N-heterocycles are more strongly bound than the S-heterocycles, which are more strongly bound than O-heterocycles. On Pd surfaces, experimental measurement of desorption energy of heterocycles is complicated by C-heteroatom cleavage,[80] but the same order of heterocycle binding affinity has been reported with thermal desorption spectroscopy of pyrrole, thiophene, and furan on Cu(100).[81]

Sterics play a role in binding affinity to dipalladium(I). Substitution of the thiophenes and furans weakens binding, but only by less than one order of magnitude. This effect is likely due to steric repulsion between the heterocycle substituents and phosphine groups. In the case of 4,6-Me_2-DBT, the substitution precludes π-binding, and the resulting μ^2-S binding is so weak (10^4 fold weaker than thiophene) that an equilibrium constant could not be determined directly against **7** but had to be determined against toluene adduct **3** instead.

NIH-PA Author Manuscript

NIH-PA Author Manuscript

NIH-PA Author Manuscript

THT quantitatively displaces thiophene from **7**, so its relative binding affinity was determined against the *N*-methylpyrrole adduct **12**. Similarly, butadiene quantitatively displaces *N*-methylpyrrole from **12**, therefore its binding affinity was determined against THT, and that of CHD, the strongest binding neutral ligand in this study, was determined relative to butadiene. Because of broadening of ^{1}H NMR signals and the overlapping of other ^{1}H NMR features, equilibria involving THT and **18** (vs *N*-methylpyrrole and butadiene) were determined by integration of ^{31}P NMR spectra.

Exposure of allyl adduct **20** to 4 atm butadiene did not induce any reaction. Anionic ligands are probably not displaced by neutral ligands for Coulombic reasons. Allyl is thus very tightly bound to dipalladium(I) and could not be quantitatively placed on the relative binding affinity scale.

Two potential ligands which did not measurably react with toluene adduct **3** were tetrahydrofuran and PI1CF_3, even at 100 equivalents. A benzaldehyde adduct was observed in equilibrium with **3** by NMR in CD_3NO_2 (^{1}H: 9.38 ppm, s, C*H*O vs 9.99 ppm for free benzaldehyde; ^{31}P: 70.2 ppm, s), but could not be isolated. Compared to toluene, electron deficient benzaldehyde binds *ca*. 1000 times more weakly, while more electron rich anisole bind greater than 10 times more strongly.

2.7. Computational Guide to Relative Binding Affinities

The observed relative binding affinity of arenes (PhOMe, PhMe, PhCHO, $PhCF_3$) is correlated with arene electron-richness, which has been tabulated for various substituted benzenes usin, empirically-derived Hammett parameters or related resonance effect parameters (e.g., σ_p or *R*).[82]

The strong binding of pyrrole mirrors the greater electron density of pyrrole relative to thiophene and furan. For example, weak electrophiles such as benzenediazonium cation and nitrous acid are known to induce rapid electrophilic aromatic substitution with pyrrole but do not react with thiophene and furan.[69] Qualitatively, electrostatic potential (ESP) plots reveal the regions of greatest electron density in the ground state of heterocycles, and have been predictive for cation-π interactions.[83,84] The ESPs of pyrrole, thiophene, furan, indole, and benzothiophene were mapped onto their molecular electron density isosurfaces (Figure 5) using the GaussView program.[85] As expected, pyrrole has the most electron-rich (red) π-system. While ESPs of thiophene and furan look similar to each other, the electron density of thiophene is spread across the four binding carbons, whereas in furan, the alpha carbons are less electron rich (yellow/green), accounting for furan's weaker binding affinity. Previous studies of Na^{+}-π interactions found the same trend in binding affinity and ESPs for pyrrole, thiophene, and furan.[84]

The ESPs at the η^3- vs η^4-binding sites of indole and benzothiophene predict the regioselectivity of the observed adducts. For indole, the four carbons from the carbocyclic ring have more negative charge than the three atoms from the heterocyclic ring, while for benzothiophene, the heterocyclic ring is less positively charged (blue) than the carbocyclic ring. These contrasting electron distributions are reflected in the observed complementary binding modes of indole and benzothiophene. Previous studies of cation-indole (or tryptophan) interactions have also found preferential binding to the carbocyclic ring.[83] However, the electrostatic potential of benzothiophene has not previously been discussed in the context of cation-π–system binding. Although pure Pd(0) would not be expected to exhibit significant electrostatic interactions, palladium sulfides or hydrides present during catalysis may induce surface polarization[86] and, subsequently, cation-π-like interactions.

NIH-PA Author Manuscript

NIH-PA Author Manuscript

NIH-PA Author Manuscript

2.8. Molecular Orbital Interactions in μ-η^2:η^2 Binding

Although simple electrostatics can be predictive for similar ligands in these complexes (*vide supra*), the interactions between the dipalladium unit and a capping diene have a covalent component as described by bonding molecular orbitals derived from Pd d-orbitals and diene π-system. The μ-η^2:η^2-binding mode of two π-systems in sandwich dipalladium(I) complexes has been previously examined by others.[6,19,87] Diene binding is described through two key interactions: donation of the diene HOMO to the Pd–Pd [dσ–dσ]* antibonding orbital (Figure 6a) and back-donation of the Pd–Pd dσ–dσ bonding orbital to the diene LUMO (Figure 6b).

This established bonding model was compared with DFT calculations of a series of model complexes of the form $[Pd_2L(\mu\text{-}\eta^2\text{:}\eta^2\text{-ligand})]^{2+}$ (L = Me-for-^{i}Pr variant of **1**; ligand = benzene, s-*trans*-butadiene, 1,3-cyclohexadiene, thiophene, furan) and $[Pd_2L(allyl)]^+$. For illustrative purposes, select MOs from the benzene, butadiene, and thiophene adducts are presented in Figure 7 (for other complexes, see Supporting Information, Figure S41). The ligand-HOMO-to-[dσ–dσ]* donation is consistent across all of the complexes (Figure 7, left). However, the constitution of the Pd_2-to-ligand back-bond varies.

The LUMO of a generic s-*cis*-diene is symmetric with respect to reflection in the plane perpendicular to the molecule (i.e. transforms as the a' irreducible representation in the C_s point group). There are six filled metal/phosphine-based frontier orbitals for the $[Pd_2L]^{2+}$ fragment of the same symmetry (Figure S40), and any of these could back-donate into the diene LUMO. The dσ–dσ orbital has the best energy match to donate to a ligand-based orbital, and indeed is observed participating in a strong interaction in $[Pd_2L(allyl)]^+$ (Figure S41). For dienes, however, the dσ–dσ lobes are directed at nodes in the diene LUMO. Instead, the primary metal-based orbital for back-donation to dienes has dπ–dπ character, as seen with s-*trans*-butadiene (Figure 6c; Figure 7, middle right). For s-*cis*-dienes (e.g. benzene, thiophene), some dδ–dδ character is also mixed into the back-bonding interaction to accommodate the arrangement of the diene LUMO (Figure 6d; Figure 7, right).

3. Conclusions

A novel dipalladium(I) terphenyl diphosphine framework has been used to study well-defined π-bound complexes of toluene, anisole, 1,3-butadiene, 1,3-cyclohexadiene, thiophenes, pyrroles, and furans across two metal centers using crystallography, NMR spectroscopy, and DFT. σ-bound complexes of tetrahydrothiophene and 4,6-dimethyldibenzothiophene and π-complexes of allyl and diacetonitrilyl anions are also described. Of note, the first crystallographically characterized μ-η^2:η^2 1,3-cyclohexadiene, thiophene, and furan adducts and μ-η^2:η^1(S) benzothiophene adduct are reported. The thiophene and benzothiophene adducts undergo hydrogenation to yield tetrahydrothiophene and dihydrobenzothiophene adducts. Unlike in previous systems, the multidentate framework allows substitution of only one bridging ligand, or a single molecular hemisphere. The resulting asymmetry of the complex allows for analysis of bonding dynamics by NMR spectroscopy. Capping aromatics and thiophenes undergo rapid flipping or spinning processes at room temperature, while such processes are slow for 1,3-cyclohexadiene, pyrrole, furan, and allyl ligands. Importantly, the common binding framework also allows for determination of relative binding strengths by NMR spectroscopy. Competition experiments revealed a scale of relative binding affinities spanning over 13 orders of magnitude. The general trends observed in this study were found to relate to the electron density of the π-systems. Increasing binding affinity in the order furan < thiophene < pyrrole is rationalized based on the electrostatic potentials at the binding atoms. Complementary binding modes of benzothiophene and indole are also explained through similar analysis. Unlike pure cation-π interactions, these binding interactions are

NIH-PA Author Manuscript

NIH-PA Author Manuscript

NIH-PA Author Manuscript

shown by DFT calculations to involve Pd-Pd dσ–dσ, dπ–dπ, and dδ–dδ orbitals. Overall, the present system offers a platform to study binding and reactivity at two adjacent metal centers. To our knowledge this is the only system that has afforded quantitative determination of relative equilibrium binding affinities for a wide variety of organic molecules coordinating via π-systems to transition metal centers. These studies provide structural, thermodynamic, and electronic insight into the binding of such substrates to homogeneous or heterogeneous bimetallic sites.

Supplementary Material

Refer to Web version on PubMed Central for supplementary material.

Acknowledgments

We thank Aaron Sattler for helpful discussion and Lawrence M. Henling and Jens Kaiser for assistance with collection of crystallographic data. We are grateful to Caltech, BP, NSF CAREER CHE-1151918, and NSF GRFP (S.L.) for funding. We thank the Gordon and Betty Moore Foundation for their generous support of the Molecular Observatory at Caltech. The Bruker KAPPA APEXII X-ray diffractometer was purchased via an NSF CRIF:MU Award to Caltech (Grant No. CHE-0639094). The 400 MHz NMR spectrometer was purchased via an NIH award (No. RR027690).

REFERENCES

(1). Hafner J. Monatsh. Chem. 2008; 139:373.

(2). Biffis A, Zecca M, Basato M. J. Mol. Catal. A: Chem. 2001; 173:249.

(3). Augustine RL, O'Leary ST. J. Mol. Catal. A: Chem. 1995; 95:277.

(4). Prins R, Egorova M, Röthlisberger A, Zhao Y, Sivasankar N, Kukula P. Catal. Today. 2006; 111:84.

(5). Girgis MJ, Gates BC. Ind. Eng. Chem. Res. 1991; 30:2021.

(6). Murahashi T, Kimura S, Takase K, Ogoshi S, Yamamoto K. Chem. Commun. 2013; 49:4310.

(7). Murahashi T, Nagai T, Okuno T, Matsutani T, Kurosawa H. Chem. Commun. 2000:1689.

(8). Murahashi T, Kurosawa H. Coord. Chem. Rev. 2002; 231:207.

(9). Paton RS, Brown JM. Angew. Chem Int. Ed. 2012; 51:10448.

(10). Allegra G, Tettamanti Casagrande G. Immirzi A, Porri L, Vitulli G. J. Am. Chem. Soc. 1970; 92:289.

(11). Dupont J, Pfeffer M, Rotteveel MA, De Cian A, Fischer J. Organometallics. 1989; 8:1116.

(12). Sommovigo M, Pasquali M, Leoni P, Braga D, Sabatino P. Chem. Ber. 1991; 124:97.

(13). Åkerstedt J, Gorlov M, Fischer A, Kloo L. J. Organomet. Chem. 2010; 695:1513.

(14). Dotta P, Kumar PGA, Pregosin PS, Albinati A, Rizzato S. Organometallics. 2004; 23:4247.

(15). Barder TE. J. Am. Chem. Soc. 2005; 128:898. [PubMed: 16417380]

(16). Christmann U, Pantazis DA, Benet-Buchholz J, McGrady JE, Maseras F, Vilar R. n. J. Am. Chem. Soc. 2006; 128:6376. [PubMed: 16683802]

(17). Murahashi T, Takase K, Oka M, Ogoshi S. J. Am. Chem. Soc. 2011; 133:14908. [PubMed: 21848326]

(18). Murahashi T, Fujimoto M, Oka M, Hashimoto Y, Uemura T, Tatsumi Y, Nakao Y, Ikeda A, Sakaki S, Kurosawa H. Science. 2006; 313:1104. [PubMed: 16931758]

(19). Murahashi T, Otani T, Mochizuki E, Kai Y, Kurosawa H, Sakaki S. J. Am. Chem. Soc. 1998; 120:4536.

(20). Murahashi T, Kanehisa N, Kai Y, Otani T, Kurosawa H. Chem. Commun. 1996:825.

(21). Leoni P, Pasquali M, Sommovigo M, Albinati A, Lianza F, Pregosin PS, Ruegger H. Organometallics. 1993; 12:4503.

(22). Werner H, Kühn A, Tune DJ, Krüger C, Brauer DJ, Sekutowski JC, Tsay Y.-h. Chem. Ber. 1977; 110:1763.

NIH-PA Author Manuscript

NIH-PA Author Manuscript

NIH-PA Author Manuscript

(23). Werner H, Kraus H-J, Schubert U, Ackermann K. Chem. Ber. 1982; 115:2905.
(24). Hruszkewycz DP, Wu J, Hazari N, Incarvito CD. J. Am. Chem. Soc. 2011; 133:3280. [PubMed: 21329388]
(25). Kobayashi Y, Iitaka Y, Yamazaki H. Acta Crystallogr. Sect. B. 1972; 28:899.
(26). Sui-Seng C, Enright GD, Zargarian D. J. Am. Chem. Soc. 2006; 128:6508. [PubMed: 16683817]
(27). Markert C, Neuburger M, Kulicke K, Meuwly M, Pfaltz A. Angew. Chem. Int. Ed. 2007; 46:5892.
(28). Velian A, Lin S, Miller AJM, Day MW, Agapie T. J. Am. Chem. Soc. 2010; 132:6296. [PubMed: 20397653]
(29). Lin S, Day MW, Agapie T. J. Am. Chem. Soc. 2011; 133:3828. [PubMed: 21344904]
(30). Chao ST, Lara NC, Lin S, Day MW, Agapie T. Angew. Chem. Int. Ed. 2011; 50:7529.
(31). Kelley P, Lin S, Edouard G, Day MW, Agapie T. J. Am. Chem. Soc. 2012; 134:5480. [PubMed: 22394331]
(32). Kaye, GWC.; Laby, TH. Tables of Physical and Chemical Constants. 15th ed. Longmon; London, UK: 1993.
(33). Efremenko I. J. Mol. Catal. A: Chem. 2001; 173:19.
(34). Brandenburg, K. DIAMOND. Crystal Impact GbR; Bonn, Germany: 1999.
(35). Fulmer GR, Miller AJM, Sherden NH, Gottlieb HE, Nudelman A, Stoltz BM, Bercaw JE, Goldberg KI. Organometallics. 2010; 29:2176.
(36). Katano S, Ichihara S, Ogasawara H, Kato HS, Komeda T, Kawai M, Domen K. Surf. Sci. 2002; 502-503:164.
(37). Murahashi T, Kurosawa H. J. Organomet. Chem. 1999; 574:142.
(38). Reiß GJ, Konietzny S. J. Chem. Soc., Dalton Trans. 2002:862.
(39). Tatsumi Y, Naga T, Nakashima H, Murahashi T, Kurosawa H. Chem. Commun. 2004:1430.
(40). The unusual downfield-shifted multiplet was confirmed to belong to the bridging diene by two-dimensional ^{1}H-^{1}H NMR correlation spectroscopy (COSY). This feature is consistently found in **5-8** as the protons bound to the two carbons of the diene closest to Pd. The protons bound to the two internal carbons of the diene moiety are consistently shifted upfield.
(41). Saeys M, Reyniers MF, Neurock M, Marin GB. Surf. Sci. 2006; 600:3121.
(42). Harshbarger WR, Bauer SH. Acta Crystallogr. Sect. B. 1970; 26:1010.
(43). Harman WD. Coord. Chem. Rev. 2004; 248:853.
(44). Keane JM, Harman WD. Organometallics. 2005; 24:1786.
(45). Delafuente DA, Myers WH, Sabat M, Harman WD. Organometallics. 2005; 24:1876.
(46). Ateşin TA, Jones WD. Organometallics. 2007; 27:53.
(47). Ateşin TA, Jones WD. Organometallics. 2008; 27:3666.
(48). Hachgenei JW, Angelici R. J. Organometallics. 1989; 8:14.
(49). Angelici R. J. Organometallics. 2001; 20:1259.
(50). Janak KE, Tanski JM, Churchill DG, Parkin G. J. Am. Chem. Soc. 2002; 124:4182. [PubMed: 11960426]
(51). Sattler A, Janak KE, Parkin G. Inorg. Chim. Acta. 2011; 369:197.
(52). Vicic DA, Jones WD. J. Am. Chem. Soc. 1999; 121:7606.
(53). Jones WD, Chin RM, Hoaglin CL. Organometallics. 1999; 18:1786.
(54). Jones WD, Chin RM. Organometallics. 1992; 11:2698.
(55). Capon J-F, Schollhammer P, Pétillon F. o. Y. Talarmin J, Muir KW. Organometallics. 1999; 18:2055.
(56). Grochowski MR, Li T, Brennessel WW, Jones WD. J. Am. Chem. Soc. 2010; 132:12412. [PubMed: 20704269]
(57). Iovu MC, Sheina EE, Gil RR, McCullough RD. Macromolecules. 2005; 38:8649.
(58). Terada S, Yokoyama T, Sakano M, Imanishi A, Kitajima Y, Kiguchi M, Okamoto Y, Ohta T. Surf. Sci. 1998; 414:107.
(59). Schwalbe M, Walther D, Schreer H, Langer J, Görls H. J. Organomet. Chem. 2006; 691:4868.

NIH-PA Author Manuscript

NIH-PA Author Manuscript

NIH-PA Author Manuscript

(60). Orita H, Itoh N. Surf. Sci. 2004; 550:177.

(61). Such a motif (with S bound to a third metal) has been proposed in a DFT study of thiophene on Pt(111): Zhu H, Guo W, Li M, Zhao L, Li S, Li Y, Lu X, Shan H. ACS Catal. 2011; 1:1498.

(62). Adams RD, Qu X. Organometallics. 1995; 14:2238.

(63). Kabir SE, Miah MA, Sarker NC, Golzar Hussain GM, Hardcastle KI, Nordlander E, Rosenberg E. Organometallics. 2005; 24:3315.

(64). The ^{1}H NMR multiplet at 8.80 ppm was absent when **3** was treated with 2,5-d^{2}-thiophene.

(65). Knight MJ, Allegretti F, Kröger EA, Polcik M, Lamont CLA, Woodruff DP. Surf. Sci. 2008; 602:2524.

(66). Wang H, Prins R. J. Catal. 2009; 264:31.

(67). Meille V, Schulz E, Lemaire M, Faure R, Vrinat M. Tetrahedron. 1996; 52:3953.

(68). Pearson RG. J. Am. Chem. Soc. 1963; 85:3533.

(69). Joule, JA.; Mills, K. Heterocyclic Chemistry. 4th ed. Blackwell Publishing; Ames, Iowa: 2000.

(70). Stanislaus A, Marafi A, Rana MS. Catal. Today. 2010; 153:1.

(71). Fu W, Zhang L, Tang T, Ke Q, Wang S, Hu J, Fang G, Li J, Xiao F-S. J. Am. Chem. Soc. 2011; 133:15346. [PubMed: 21913690]

(72). Yu K, Li H, Watson EJ, Virkaitis KL, Carpenter GB, Sweigart DA. Organometallics. 2001; 20:3550.

(73). Baldovino-Medrano VG, Giraldo SA, Centeno A. b. J. Mol. Catal. A: Chem. 2009; 301:127.

(74). Mozingo R, Harris SA, Wolf DE, Hoffhine CE, Easton NR, Folkers K. J. Am. Chem. Soc. 1945; 67:2092. [PubMed: 21005673]

(75). Rooney JJ, Gault FG, Kemball C. Proc. Chem. Soc. 1960:407.

(76). Hruszkewycz DP, Wu J, Green JC, Hazari N, Schmeier T. J. Organometallics. 2011; 31:470.

(77). Avent AG, Frankland AD, Hitchcock PB, Lappert MF. Chem. Commun. 1996:2433.

(78). A similar (deprotonated) tautotmer and binding motif has been reported bound to a phosphido-palladium two-centered moiety: Braunstein P, Matt D, Dusausoy Y, Fischer J. Organometallics. 1983; 2:1410.

(79). Ligand exchange kinetics have been studied for π-adducts of mononuclear d^{6} octahedral compounds, but thermodynamic binding experiments have not been reported to the authors' knowledge. See: Mocella CJ, Delafuente DA, Keane JM, Warner GR, Friedman LA, Sabat M, Harman WD. Organometallics. 2004; 23:3772–3779.

(80). Caldwell TE, Land DP. Polyhedron. 1997; 16:3197.

(81). Sexton BA. Surf. Sci. 1985; 163:99.

(82). Hansch C, Leo A, Taft RW. Chem. Rev. 1991; 91:165.

(83). Mecozzi S, West AP, Dougherty DA. Proc. Watl. Acad. Sci. USA. 1996; 93:10566.

(84). Ma JC, Dougherty DA. Chem. Rev. 1997; 97:1303. [PubMed: 11851453]

(85). Gaussian 09, Revision C.01, Frisch MJ, Trucks GW, Schlegel HB, Scuseria GE, Robb MA, Cheeseman JR, Scalmani G, Barone V, Mennucci B, Petersson GA, Nakatsuji H, Caricato M, Li X, Hratchian HP, Izmaylov AF, Bloino J, Zheng G, Sonnenberg JL, Hada M, Ehara M, Toyota K, Fukuda R, Hasegawa J, Ishida M, Nakajima T, Honda Y, Kitao O, Nakai H, Vreven T, Montgomery Jr., J. A. Peralta JE, Ogliaro F, Bearpark M, Heyd JJ, Brothers E, Kudin KN, Staroverov VN, Kobayashi R, Normand J, Raghavachari K, Rendell A, Burant JC, Iyengar SS, Tomasi J, Cossi M, Rega N, Millam JM, Klene M, Knox JE, Cross JB, Bakken V, Adamo C, Jaramillo J, Gomperts R, Stratmann RE, Yazyev O, Austin AJ, Cammi R, Pomelli C, Ochterski JW, Martin RL, Morokuma K, Zakrzewski VG, Voth GA, Salvador P, Dannenberg JJ, Dapprich S, Daniels AD, Farkas Ö, Foresman JB, Ortiz JV, Cioslowski J, Fox DJ. 2009Gaussian, Inc.Wallingford CT

(86). Theoretical study of chemisorbed H on Pd surfaces suggests that formation of an H—Pd bond is accompanied by transfer of *ca*. 0.2 electrons from Pd to H. See: Tománek D, Sun Z, Louie SG. Physical Review B. 1991; 43:4699–4713.

(87). Kurosawa H. J. Organomet. Chem. 2004; 689:4511.

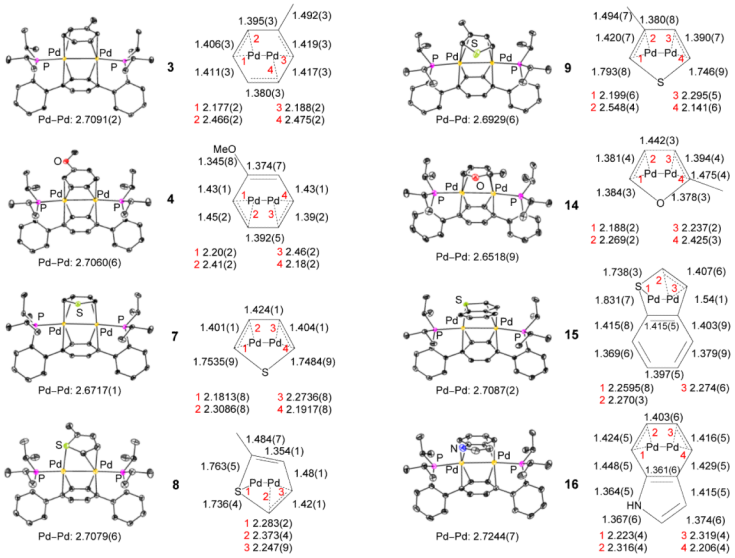

Figure 1.

Structures of **3**, **4**, **7-9**, **14-16** as determined by single-crystal X-ray diffraction. Thermal ellipsoids generated at the 50% probability level.[34] Outer-sphere anions, solvent molecules, and hydrogen atoms are not shown. Bond distances (Å) for the capping ligands are shown.

NIH-PA Author Manuscript NIH-PA Author Manuscript NIH-PA Author Manuscript

NIH-PA Author Manuscript

NIH-PA Author Manuscript

NIH-PA Author Manuscript

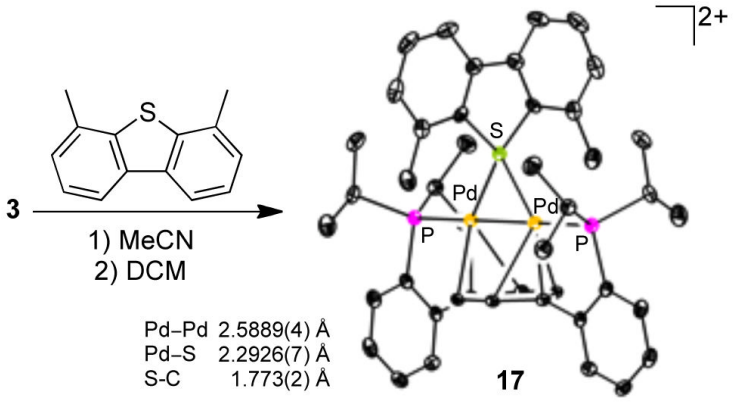

Figure 2.
Synthesis and solid-state structure of 4,6-dimethyldibenzothiophene adduct **17** with 50% thermal ellipsoids. Outer-sphere anions, solvent molecules, and hydrogen atoms not shown.

NIH-PA Author Manuscript

NIH-PA Author Manuscript

NIH-PA Author Manuscript

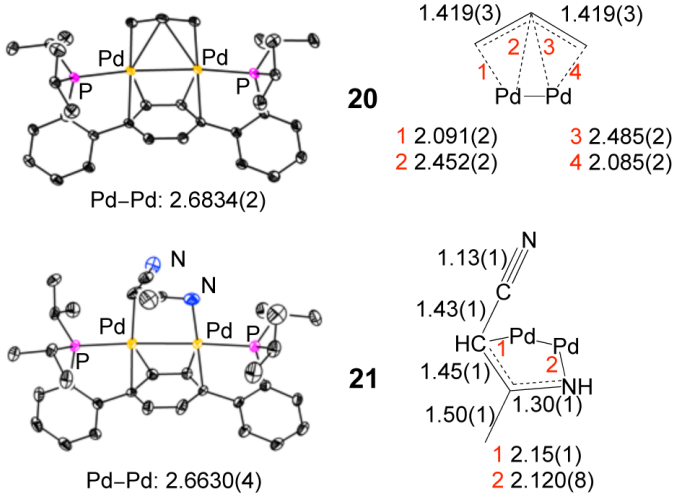

Figure 3.

Structures of **20** and **21** as determined by singlecrystal x-ray diffraction, with 50% prob. thermal ellipsoids. Outer-sphere anions, solvent molecules, and hydrogen atoms are not shown. Bond distances for the capping ligands are shown.

NIH-PA Author Manuscript

NIH-PA Author Manuscript

NIH-PA Author Manuscript

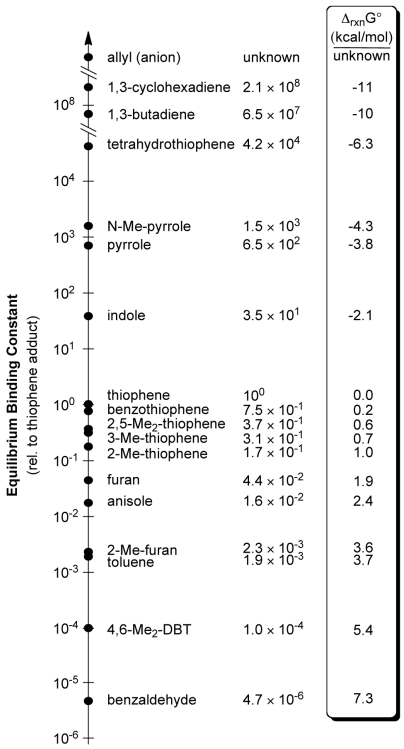

Figure 4.
Equilibrium binding constants and relative standard Gibbs free energy of reaction of various arenes and heterocycles (eq 2).

NIH-PA Author Manuscript

NIH-PA Author Manuscript

NIH-PA Author Manuscript

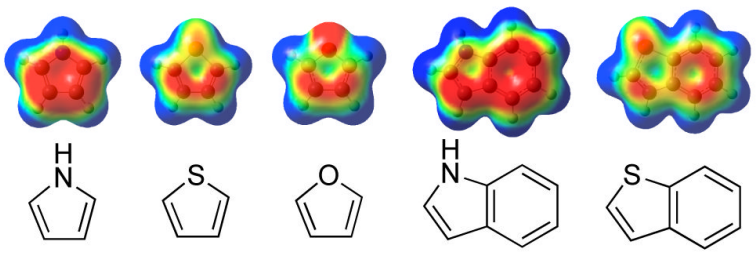

Figure 5.
Electrostatic potentials (above) plotted onto electron density isosurfaces (isovalue = 0.004) of of unbound heterocycles (below). Red represents a potential energy lower or equal to −0.02 Hartrees (electron-rich), and blue a potential energy higher or equal to +0.02 Hartrees (electronpoor).

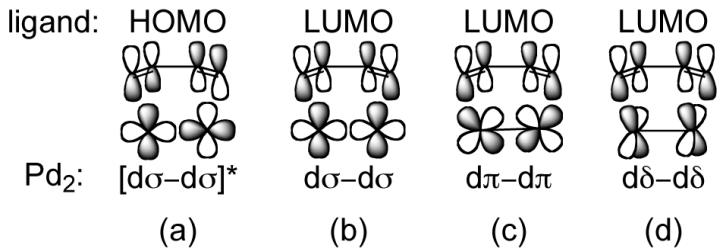

Figure 6.
Bonding interactions between (a) diene HOMO and unfilled Pd_2-based orbital and (b-d) diene LUMO and filled Pd_2-based orbitals.

NIH-PA Author Manuscript
NIH-PA Author Manuscript
NIH-PA Author Manuscript

NIH-PA Author Manuscript

NIH-PA Author Manuscript

NIH-PA Author Manuscript

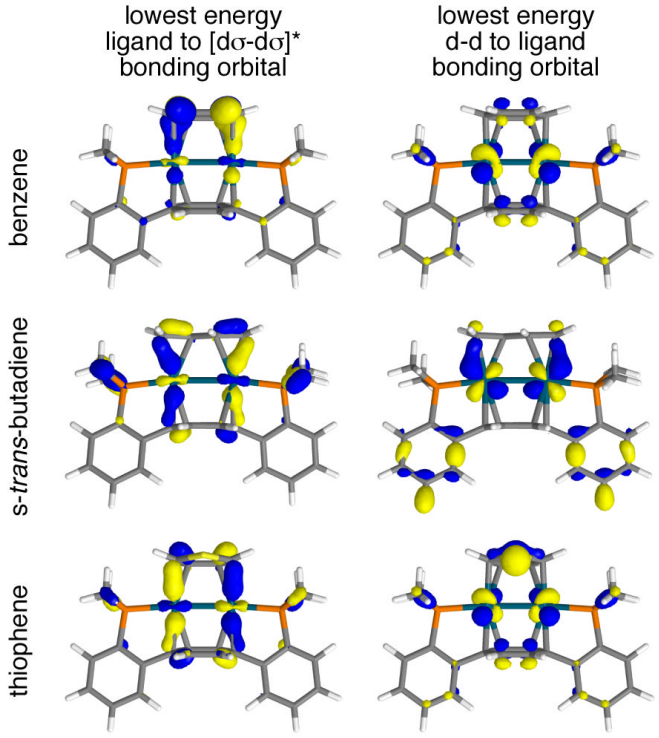

Figure 7.
Lowest energy Pd_2-ligand bonding orbitals (isosurface = 0.05) with [dσ–dσ]* Pd_2 component (left) and mixed dπ–dπ/dδ–dδ Pd_2 component (right). Lower energy molecular orbitals involving less than 20% Pd_2 contribution are not shown.

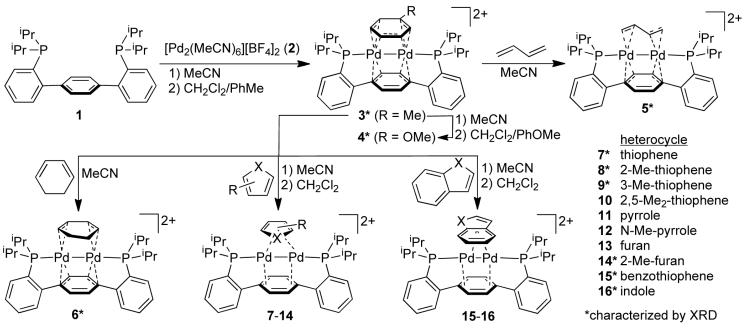

Scheme 1.

Synthesis of dipalladium(I) diphosphine compounds 3-16. Dicationic complexes 3-16 have BF_4 counterions.

NIH-PA Author Manuscript NIH-PA Author Manuscript NIH-PA Author Manuscript

NIH-PA Author Manuscript

NIH-PA Author Manuscript

NIH-PA Author Manuscript

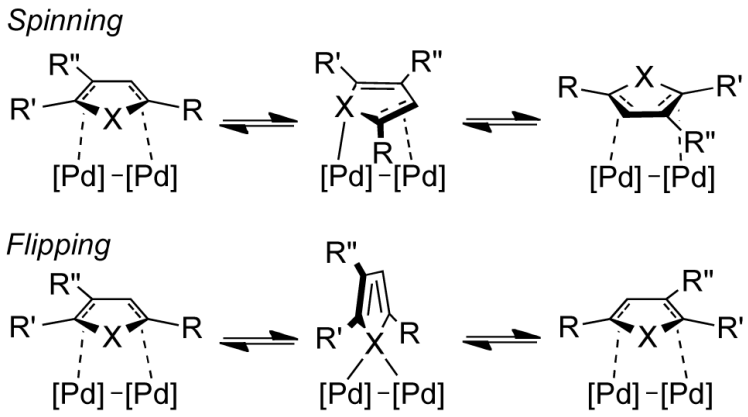

Scheme 2.
Fluxional processes for heterocycle adducts

NIH-PA Author Manuscript

NIH-PA Author Manuscript

NIH-PA Author Manuscript

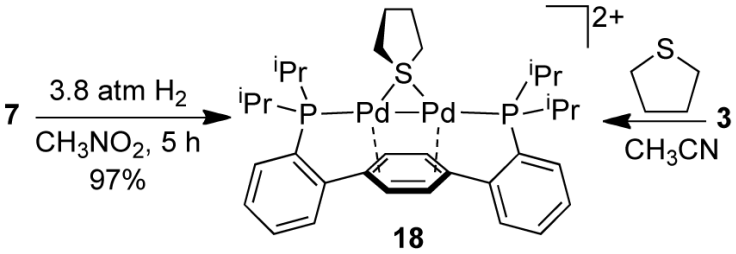

Scheme 3.
Hydrogenation and direct routes to tetrahydrothiophene adduct 18

NIH-PA Author Manuscript

NIH-PA Author Manuscript

NIH-PA Author Manuscript

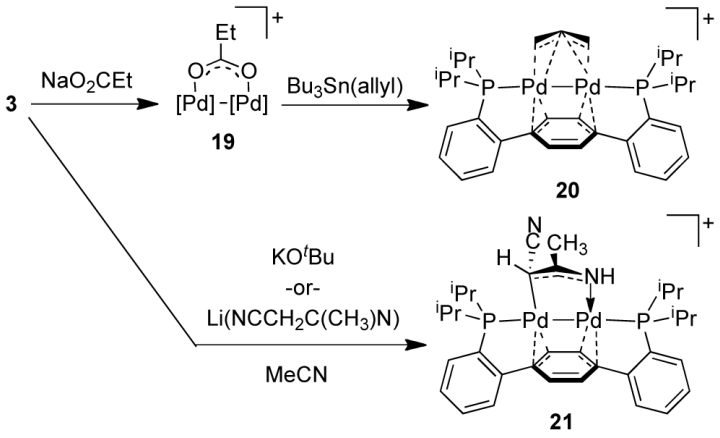

Scheme 4.
Synthesis of allyl species 20 and heteroallyl species 21.

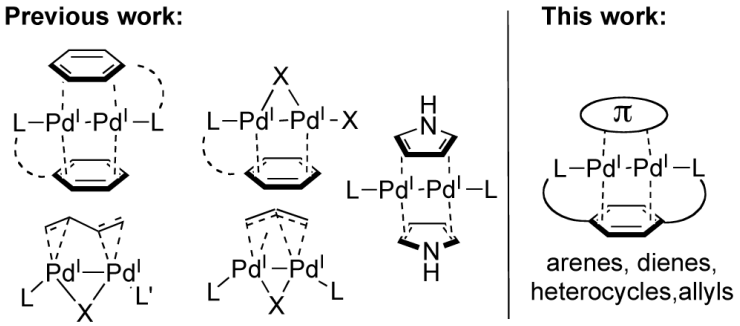

Chart 1.

Representations of dipalladium(I) compounds. Dashed arcs indicate ligands with or without covalent linkages.

NIH-PA Author Manuscript NIH-PA Author Manuscript NIH-PA Author Manuscript